Electronic Supplementary Material (ESI) for ChemComm.


# Supporting Information

# Flame-made $Cu/ZrO_2$ Catalysts with Metastable Phase and Strengthened Interactions for $CO_2$ Hydrogenation to Methanol

Meng Yang[a,b], Jiafeng Yu[a,*], Xin Tong[a,b], Xingtao Sun[a,b], Hengyong Xu[a], Jian Sun[a,*]

[a]Dalian Institute of Chemical Physics, Chinese Academy of Sciences, Dalian 116023, Liaoning, China

[b]University of Chinese Academy of Sciences, Beijing 100049, China

*Corresponding authors. E-mail addresses: yujf@dicp.ac.cn (Jiafeng Yu); sunj@dicp.ac.cn (Jian Sun)

## Catalysts Preparation

**Preparation of FSP-Cu/$ZrO_2$ and F-$ZrO_2$.** FSP-made Cu/$ZrO_2$ catalysts were prepared in a home-made FSP equipment with a flame generator (NanoPowder Nozzle npn) and a collection cylinder purchased from Tethis S.p.A., as described elsewhere[1]. 3.26 g copper acetate anhydrous (Aladin, Analytical Purity) and 16.15 g zirconium butoxide (Aladin, 80wt% in mineral spirits) were dissolved in a mixture of 2-ethylhexanonic acid (EHA, Aladin, Analytical Purity) and methanol (MeOH, Kermel, Analytical Purity) with volume ratio of 1:1, reaching a final metal concentration of 0.5 M. After ultrasonic treatment for 30 min, the obtained precursor solution was injected into the flame generator at a flow rate of 5 mL/min by a syringe pump (PHD ultratm, Harvard). It is then ignited instantly by the mixture of $CH_4$ (0.6 L/min) and $O_2$ (1.9 L/min). The dispersion and protection gas were $O_2$ (3.5 L/min) and air (5 L/min), respectively. On the top area of the flame, a collection cylinder and a water-cooled glass fiber filter (Whatman GF/D, 25.7 cm in diameter) was used to collect product nanoparticles by the aiding of a vacuum pump. FSP-Cu/$ZrO_2$ was 20 wt.% mass fraction of Cu in Cu/$ZrO_2$. F-$ZrO_2$ was for pure $ZrO_2$ made in the same way as FSP-Cu/$ZrO_2$. Cu content was determined to be 19.1 and 20.0 wt.% by ICP-OES and XPS, respectively (see Table S4, ESI).

**Preparation of DP-Cu/F-$ZrO_2$ and DP-Cu/C-$ZrO_2$.** These catalysts were prepared by conventional deposition method with 20 wt.% Cu loading. 3.85 g $Cu(NO_3)_2 \cdot 3H_2O$ (Kermel, Analytical Purity) was dissolved in deionized water (DI water) to form 1 M Cu cation liquid. 250 mL of 0.5 M $Na_2CO_3$ (Kermel, Analytical Purity) in DI water was also prepared. 4 g F-$ZrO_2$ was put into 200 mL DI water, then the Cu solution and $Na_2CO_3$ solution were added dropwise at the same time, keeping pH around 6.5. After Cu solution was consumed out, the mixture was continued to be stirred at 65ºC for one hour, followed by centrifugation and washed with DI water for three times, as well as dried at 120ºC overnight. The precursor without further calcination was denoted as DP-Cu/F-$ZrO_2$. DP-Cu/F-$ZrO_2$ was pretreated at 300ºC for 1 h by $H_2$ (30 mL/min) before reaction. Cu content of DP-Cu/F-$ZrO_2$ was determined to be 25.2 and 27.3 wt.% by ICP-OES and XPS, respectively (see Table S4, ESI). Cu was deposited on commercial

$ZrO_2$ powder (Beijing Beihua Fine Chemicals Co., Analytical Purity) in the same method with DP-Cu/F-$ZrO_2$ but calcined at 450ºC for 3 h, which was denoted as DP-Cu/C-$ZrO_2$.

*Catalyst Evaluation*

The activity test was performed in a high-pressure fixed-bed flow stainless steel reactor with quartz lining. 0.25 g of catalyst in 20–40 mesh was packed into the reactor. At first, the catalyst was reduced in pure $H_2$ with the rate of 30 mL/min at 300ºC for 1 h under atmospheric pressure. The reaction gas (24% $CO_2$, 72% $H_2$ and 4% $N_2$) with a flow rate of 20 mL/min was introduced into the reactor after the temperature was decreased to 50ºC. The reaction was performed at 3.0 MPa and various temperatures at 260, 240, 220 and 200ºC. The outlet gases were passed through the cold trap and then analyzed by two online gas chromatographers (GC), one is equipped with a TCD detector (SHIMADZU GC-8A) and the other is equipped with a flame ionization detector (FID, SHIMADZU GC-14C). The $CO_2$ conversion and $CH_3OH$ selectivity were obtained from the GC data.

$$X_{CO_2} = \frac{F_{CO_2,\ in} - F_{CO_2,out}}{F_{CO_2,\ in}}$$

$$S_{CH_3OH} = \frac{F_{CH_3OH,out}}{F_{CO_2,\ in} - F_{CO_2,out}}$$

$$S_{CO} = \frac{F_{CO,out}}{F_{CO_2,\ in} - F_{CO_2,out}}$$

$$methanol\ yield\ (g_{CH_3OH} \cdot kg_{Cu}^{-1} \cdot h^{-1}) = \frac{F_{CO_2} \times X_{CO_2} \times S_{CH_3OH} \times 32 \times 60}{22.4 \times m_{cat} \times x_{Cu}}$$

$X_{CO_2}$ is the conversion of $CO_2$. $S_x$ is the selectivity of x species in products. $F_{x,\ in}$ is the inlet flow rate of x species (mL/min), $F_{x,\ out}$ is the outlet flow rate of species x (mL/min). $m_{cat}$ is the amount of catalyst, $x_{Cu}$ is the Cu loading in Cu/$ZrO_2$.

*Catalyst Characterization*

The phase composition of the catalyst was identified by X-ray powder diffraction (XRD) on a PANalytical X'Pert Pro diffractometer with Cu-Kα (40 kV, 40 mA) radiation. X-ray photoelectron spectroscopy (XPS) with Auger electron spectroscopy (AES) measurements were performed by a ThermoFischer, ESCALAB 250Xi spectrometer equipped with an Al-Kα (hυ = 1486.6 eV) X-ray exciting source. The binding energies were calibrated by using the contaminant carbon (C 1s = 284.8 eV). Before Cu 2p spectra was collected, samples were etched by $Ar^+$ sputtering at 2000 eV for 30 s. XRD and XPS measurement were performed after the reduction with $H_2$ at 300ºC for 1 h and followed passivation treatment with 5% $O_2$/He at room temperature. The content of Cu in catalyst was detected by an inductively coupled plasma optical emission spectrometer (ICP-OES, PerkinElmer Optima 7300DV). The BET surface area of the catalyst were determined by $N_2$ adsorption-desorption measurement at -196ºC on a Quantachrome instrument with a pretreatment at 80ºC for 6 h under vacuum. High resolution transmission electron microscopy (HRTEM) images were obtained on a Talos200 transmission electron microscope. High-angle annular dark-field (HAADF)-STEM images of FSP-Cu/$ZrO_2$ were recorded with a HAADF detector attached in TEM. Elemental maps of Cu, O and Zr were recorded by energy dispersive X-ray (EDX) detector.

The metallic copper surface area ($S_{Cu}$) was determined by using $N_2O$ oxidant and followed by TPR according to the procedure described elsewhere[2]. The catalysts were firstly reduced in 10% $H_2$/Ar mixture (50 mL/min) with a temperature reduction program (TPR) from room temperature to 500ºC at a ramping rate of 10ºC /min. Then the reactor was purged with Ar and cooled down to room temperature. The amount of $H_2$ consumption in the first TPR was denoted as X. After that, the catalyst was exposed to 5% $N_2O/N_2$ (50 mL/min) at 50ºC for 30 min. The reactor was purged with Ar to remove the surface oxidants. Finally, the second TPR was operated in the same procedure with the first time, and $H_2$ consumption in the second TPR was denoted as Y. Dispersion ($D_{Cu}$), Cu surface area ($S_{Cu}$) and average volume-surface diameter ($d_{Cu}$) were calculated as

$$D_{Cu} = 2X / Y \times 100\%$$

$S_{Cu} = 2Y \times N_{av} / (X \times M_{Cu} \times 1.4 \times 10^{19})$

$=1353 \times Y/ X (m^2_{Cu}/g_{Cu})$

$d_{Cu} =0.5 \times X / Y$ (nm)

$N_{av}$ is Avogadro's constant;

$M_{Cu}$ is the relative atomic mass of copper (63.46 g/mol);

$1.47 \times 10^{19}$ is the number of Cu atom of per square meter

Temperature programmed desorption of $CO_2$ ($CO_2$-TPD) experiment was performed to study the $CO_2$ adsorption capacity of the catalyst. Prior to the adsorption, 50 mg of the sample was pre-reduced in $H_2$ stream at 300ºC for 1 h. After cooling down to 50ºC, the sample was exposed to a flow of 5% $CO_2$/Ar at 30ºC for 30 min for saturated adsorption, and then purged with flowing He gas at same temperature for 45 min to remove the reversibly and physically absorbed $CO_2$. Subsequently, the $CO_2$ desorption was carried out from 50 to 900ºC with a heating rate of 10ºC/min in He stream (30 mL/min). The $CO_2$ signal (m/z =44) during the desorption process was recorded by a Pfeiffer OmniStar mass spectrometer.

*In situ* diffuse-reflectance infrared Fourier transform spectroscopy (DRIFTS) results were collected on a TENSOR_II (Bruker, Germany) infrared spectrometer in diffuse reflectance FTIR (DRIFT) mode. The spectra resolution was set at 4 $cm^{-1}$. Prior to test, the powder of the catalyst was placed into an *in-situ* chamber and mounted in a quarts IR cell. Then, the sample was pretreated in 10% $H_2$/Ar flow (30 mL/min) for 30 min at 30ºC, and then the atmosphere was switched to high purity Ar flow (30 mL/min) for 30 min. After that, the sample was cooled to target temperatures and the corresponding back-ground spectra were collected for subsequent DRIFTS analysis.

To collect *in-situ* Infrared spectra of CO adsorption (CO-IR) on FSP-Cu/$ZrO_2$ and DP-Cu/F-$ZrO_2$, the samples were reduced at 300ºC for 30 min with 10% $H_2$/Ar 30 mL/min and treated with pure Ar at 300ºC and 30 mL/min for 30 min, and then cooled down to 30ºC. The back-ground spectra was collected. The gas was changed to a stream of 5% CO/He at a flow rate of 30 mL/min under atmospheric pressure for 30 min. Then the IR chamber was purged with high purity Ar for 60 min to remove gaseous CO. Finally, the time-resolved DRIFTS spectra were collected under Ar flow.

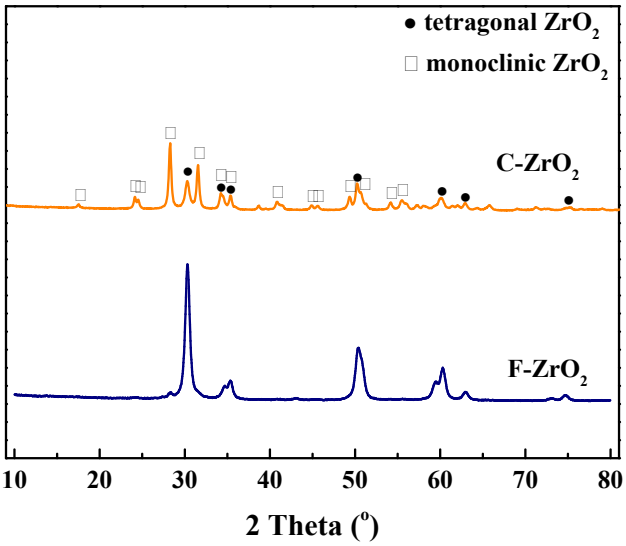


Fig. S1 XRD of commercial $ZrO_2$ and F-$ZrO_2$.

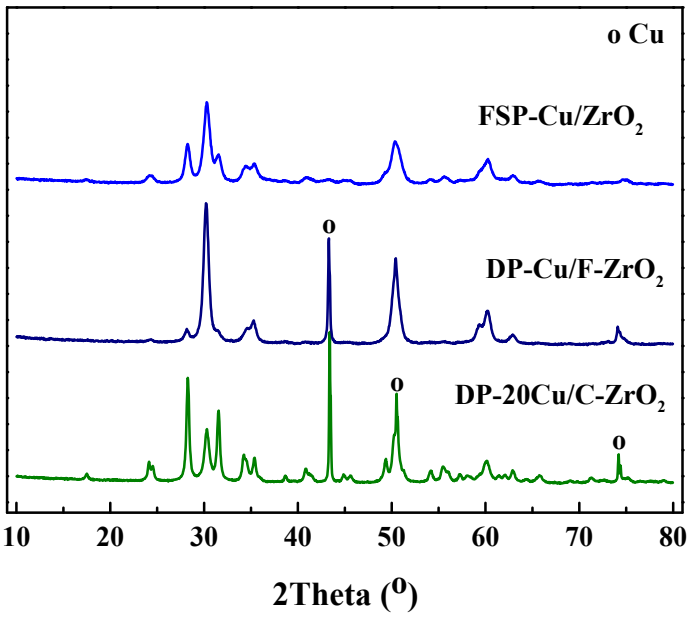


Fig. S2 XRD of all the catalysts after reduction

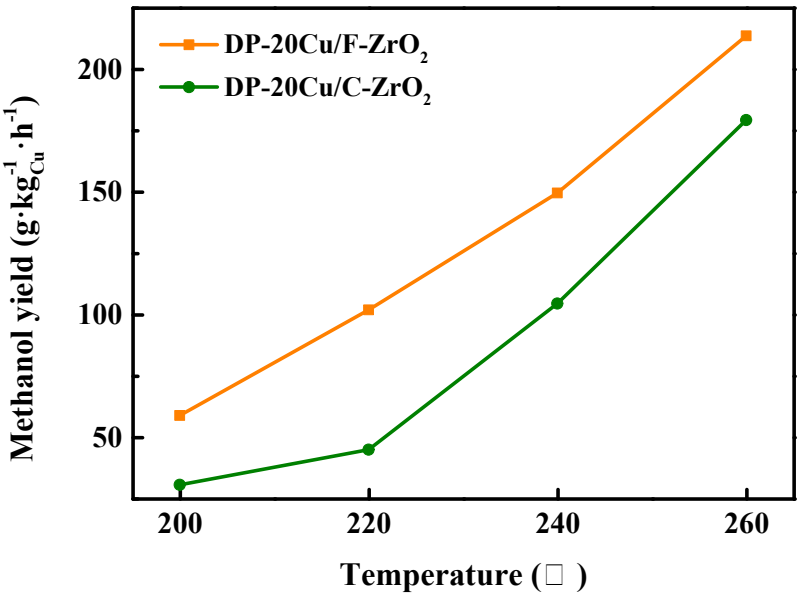


Fig. S3 Methanol yield of DP-Cu/F-$ZrO_2$ and DP-Cu/C-$ZrO_2$ at 3.0 MPa, 200-260°C, GHSV=4800 mL/($g_{cat}$·h).

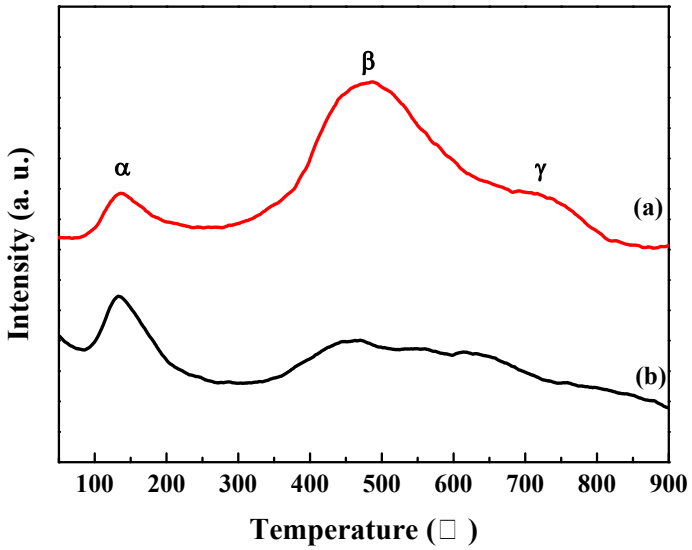


Fig. S4 $CO_2$-TPD of (a) F-$ZrO_2$ and (b) C-$ZrO_2$

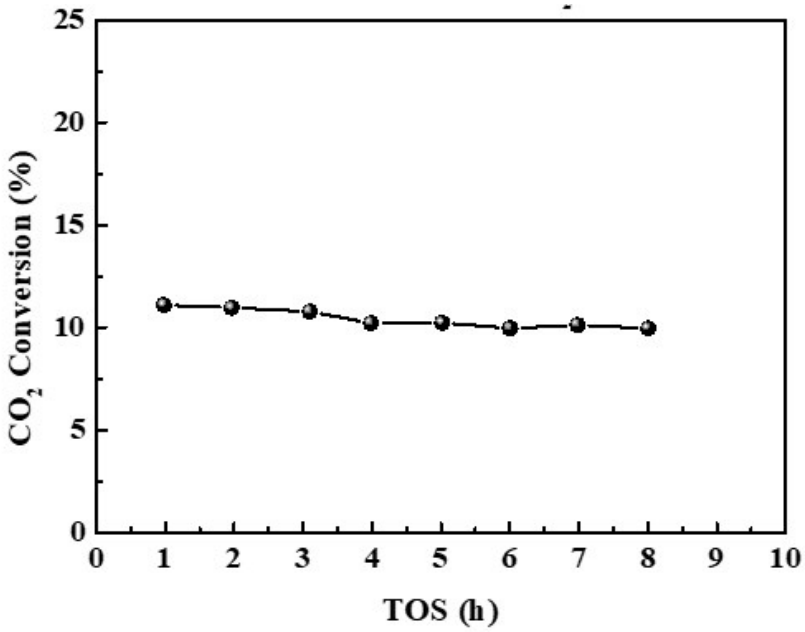


Fig. S5 Stability test of DP-Cu/F-$ZrO_2$ catalyst. Reaction condition: 260°C, 3.0 MPa and 4800 mL/($g_{cat}$·h).

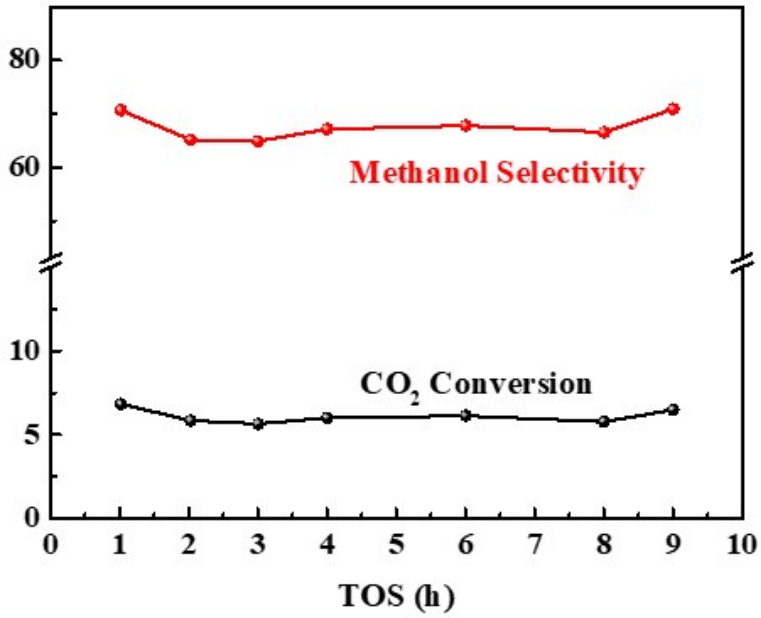


Fig. S6 Stability test of FSP-Cu/$ZrO_2$ catalyst. Reaction condition: 260°C, 3.0 MPa and 24000 mL/($g_{cat}$·h).

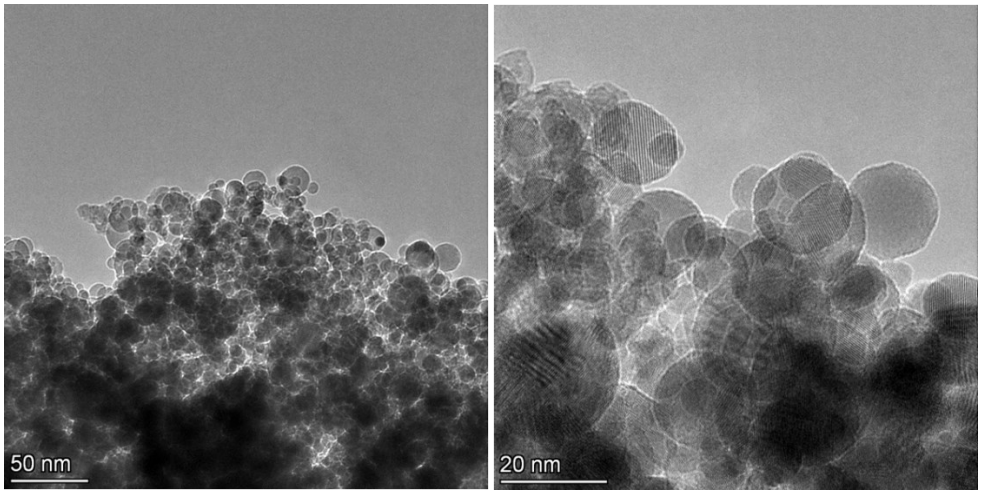


Fig. S7 HRTEM images of FSP-Cu/$ZrO_2$

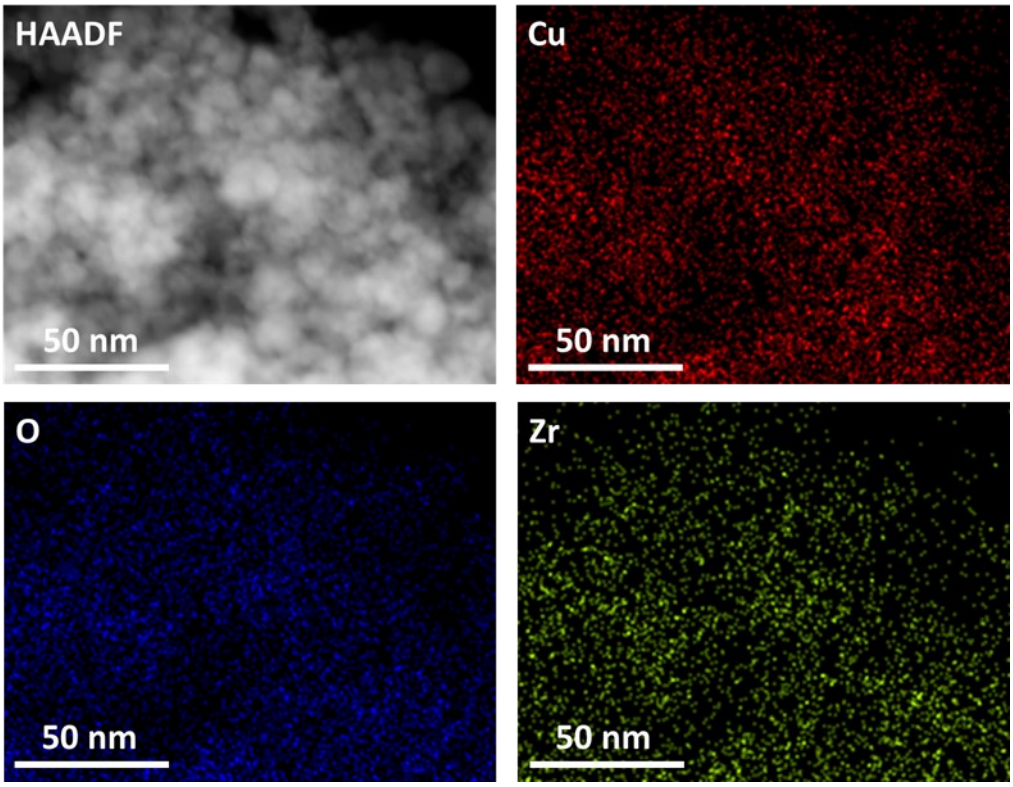


Fig. S8 HAADF-STEM images and elemental mapping of FSP-Cu/$ZrO_2$

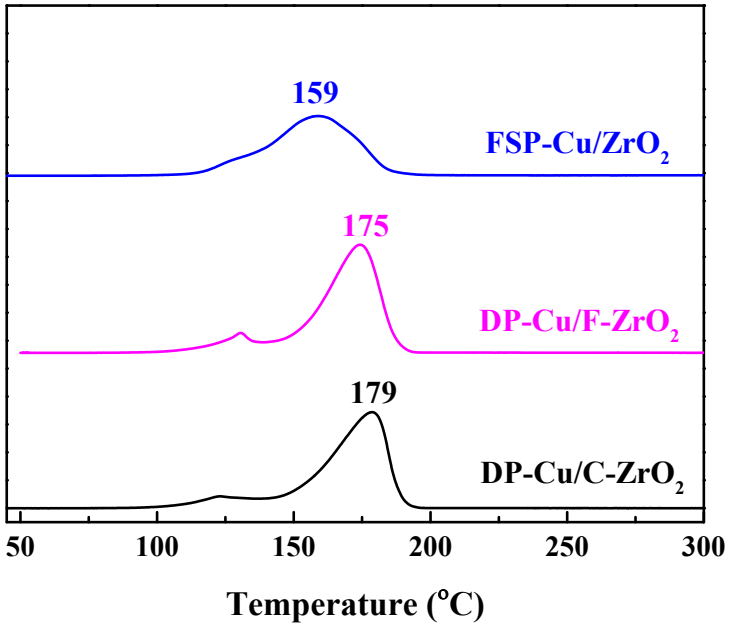


Fig. S9 $H_2$-TPR of all the tested catalysts

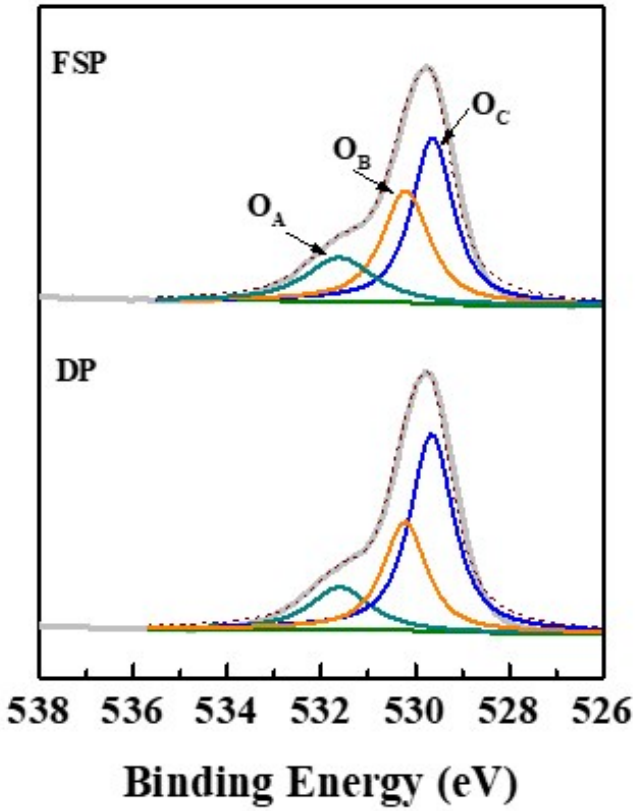


| | $O_A$(%) | $O_B$(%) | $O_C$(%) |
|---|---|---|---|
| FSP-Cu/$ZrO_2$ | 19.4 | 35.5 | 45.1 |
| DP-Cu/FSP-$ZrO_2$ | 15.6 | 29.5 | 54.9 |

Fig. S10 The XPS O 1s spectra and the percentages of each type of oxygen species of FSP-Cu/$ZrO_2$ (FSP) and DP-Cu/F-$ZrO_2$ (DP) catalysts.

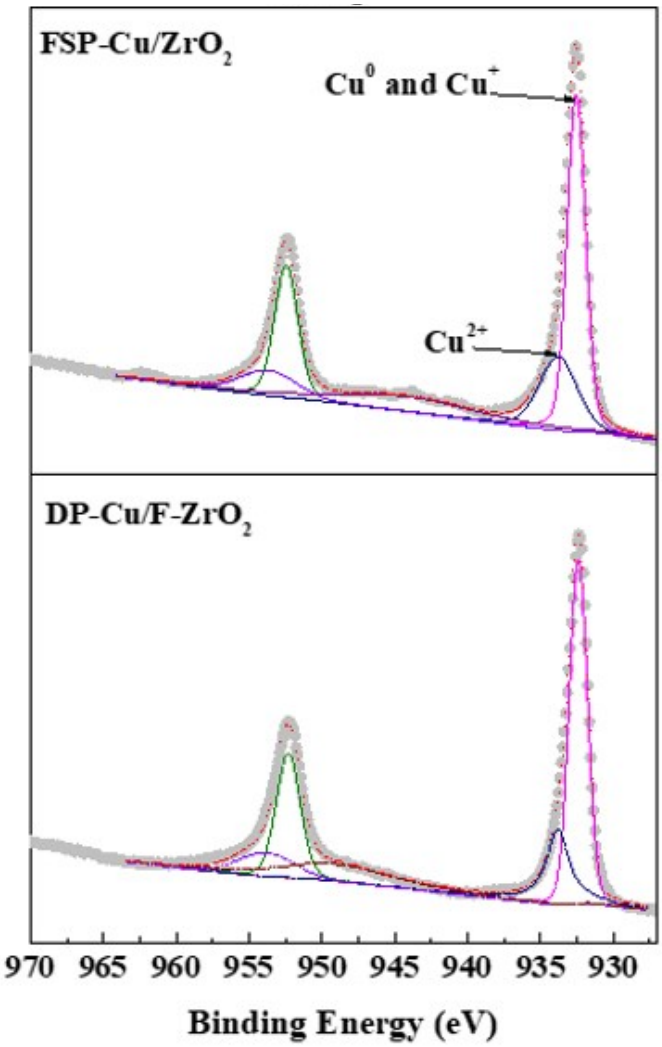


Fig. S11 The XPS Cu 2p spectra of FSP-Cu/$ZrO_2$ and DP-Cu/F-$ZrO_2$ catalysts

Table S1. Summary of infrared band of the surface species for $CO_2$+$H_2$ reaction on Cu/$ZrO_2$ and $ZrO_2$ at 0.1 MPa and 260 ºC

| Surface Species | Wavenumber ($cm^{-1}$) |
|---|---|
| Bidentate formate (bi-HCOO)[3-10] | 2967, (2879-2873), 2752, 2736, (1593-1588), 1580, (1421-1420), 1384, (1361-1360) |
| Monodentate formate (m-HCOO)[3, 4, 11] | 1560, 1295 |
| Methoxy[3, 4, 8] | (2933-2924), (2824-2820), 1147 of bridged (b-$OCH_3$), (1047-1030) of terminal (t-$OCH_3$) |
| Bidentate bicarbonate (bi-$HCO_3$)[6, 9, 11-14] | 1643, (1622-1610), 1491, (1465-1470), |
| Carbonate[12-15] | 1783, 1540, 1525, 1481, 1447, 1353, 1335-1333, (1328-1321), 1111-1107, 1106 |

Table S2. Product distributions of FSP-Cu/$ZrO_2$ and DP-Cu/F-$ZrO_2$

| Temperature (°C) | FSP-Cu/$ZrO_2$ | | | DP-Cu/F-$ZrO_2$ | | |
|---|---|---|---|---|---|---|
| | $CO_2$ Conversion (%) | Methanol Selectivity (%) | CO (%) | $CO_2$ Conversion (%) | Methanol Selectivity (%) | CO (%) |
| 260 | 13.6 | 51.9 | 49.1 | 11.4 | 37.2 | 62.8 |
| 240 | 8.3 | 64.1 | 35.9 | 5.2 | 47.8 | 52.2 |
| 220 | 5.0 | 75.8 | 24.2 | 2.6 | 61.8 | 38.2 |
| 200 | 2.4 | 85.6 | 14.4 | 1.4 | 71.6 | 28.4 |

Table S3. Comparison of catalytic performance of FSP-Cu/$ZrO_2$ in this work with other Cu/$ZrO_2$ and commercial Cu/ZnO/$Al_2O_3$ catalysts in literatures.

| Catalyst | Cu content (wt.%) | P (MPa) | T (ºC) | Methanol Selectivity (%) | $CO_2$ conversion (%) | GSHV （mL/(g·h)） | Methanol Yield (g/($g_{Cu}$·h)) |
|---|---|---|---|---|---|---|---|
| FSP-Cu/$ZrO_2$(this work) | 19.1 | 3.0 | 260 | 70.9 | 6.49 | 24000 | 2.00 |
| IM-10Cu/a-$ZrO_2$-500[16] | 10.0 | 1.0 | 230 | ca. 70.0 | ca. 0.65 | 8732 | 0.40 |
| IM-8Cu/a-$ZrO_2$-350[17] | 8.0 | 1.0 | 230 | ca. 70.0 | ca. 2.2 | 8732 | 0.56 |
| FSP-60CuO/$ZrO_2$[18] | 58.0 | 1.0 | 230 | ca. 60.0 | ca. 3.0 | 6000 | 0.05 |
| DP-10Cu@3D$ZrO_2$[19] | 12.4 | 4.5 | 260 | 78.8 | 13.1 | 21600 | 6.42 |
| DFSP-10CuO-$ZrO_2$[20] | 14.0 | 2.0 | 270 | ca. 58 | NA | 22500 | 0.60 |
| IM-10Cu/t-$ZrO_2$[21] | 10.0 | 8.0 | 260 | 86 | 15.0 | 3600 | 0.06 |
| CP-a-$ZrO_2$/90Cu [22] | 91.2 | 3.0 | 220 | 70.0 | ca. 4.0 | 48000 | 0.06 |
| CP-10Cu/$ZrO_2$[22] | 12.6 | 3.0 | 220 | ca. 75.0 | ca. 2.0 | 48000 | 1.26 |
| Cu/ZnO/$Al_2O_3$[19] | 41.8 | 4.5 | 260 | 49.7 | 22.3 | 21600 | 2.05 |

Table S4. Textural and structural properties of tested catalysts

| Catalyst | Cu content (wt.%)[b] | Surface Cu content (wt.%)[c] | Surface Area ($m^2/g$) | $S_{Cu}(m^2/g_{Cu})$[d] | $D_{Cu}(\%)$[e] | $D_{Cu}(nm)$[f] |
|---|---|---|---|---|---|---|
| FSP-Cu/$ZrO_2$ | 19.1 | 20.0 | 74.4 | 185.4 | 27.4 | 3.7 |
| DP-Cu/F-$ZrO_2$[a] | 25.2 | 27.3 | 56.2 | 24.4 | 3.6 | 27.8 |
| DP-Cu/C-$ZrO_2$ | 22.6 | – | 24.2 | 41.3 | 6.1 | 16.4 |

[a] DP-Cu/F-$ZrO_2$ are calcined at 450ºC for 3 h before $N_2O$ oxidation followed by TPR method.

[b] Determined by ICP-OES

[c] Determined by XPS

[d] Cu surface area was determined by $N_2O$ oxidation followed by TPR method.

[e] Dispersion of Cu was determined by $N_2O$ oxidation followed by TPR method.

[f] Average diameter of Cu particles was determined by $N_2O$ oxidation followed by TPR method.

## Reference


1. Z. Zhang, J. Yu, J. Zhang, Q. Ge, H. Xu, F. Dallmann, R. Dittmeyer and J. Sun, *Chem. Sci.*, 2018, **9**, 3386-3394.
2. C. J. G. V. D. Grift, A. F. H. Wielers, B. P. J. Joghi, J. V. Beijnum, M. D. Boer, M. V. Helder and J. W. Geus, *J. Catal.,* 1991, **131**, 178-189.
3. S. Posada-Perez, P. J. Ramirez, J. Evans, F. Vines, P. Liu, F. Illas and J. A. Rodriguez, *J. Am. Chem. Soc.*, 2016, **138**, 8269-8278.
4. W. Wang, Z. Qu, L. Song and Q. Fu, *J. Catal.,* 2020, **382**, 129-140.
5. N. Koizumi, G. B. l, K. Murai, T. Ozaki and M. Yamada, *J. Mol. Catal. A: Chem*., 2004, **207**, 173-182.
6. S. Bailey, *Catal. Letters*, 1995, **30**, 99-111.
7. D. Bianchi, T. Chafik, M. Khalfallah and S. J. Teichner, *Appl. Catal. A: Gen.*, 1993, **105**, 223-249.
8. S.-i. Fujita, M. Usui, E. Ohara and N. Takezawa, *Catal. Letters,* 1992, **13**, 349-358.
9. W. Hertl, *Langmuir*, 1989, **5**, 96-100.
10. Y. Amenomiya, *J. Catal.,* 1979, **57**, 64-70.
11. D. Bianchi, T. Chafik, M. Khalfallah and S. J. Teichner, *Appl. Catal. A: Gen.,* 1994, **112**, 57-73.
12. J. Weigel, R. A. Koeppel, A. Baiker and A. Wokaun, *Langmuir,* 1996, **12**, 5319-5329.
13. D. Bianchi, T. Chafik, M. Khalfallah and S. J. Teichner, *Appl. Catal. A: Gen.,* 1994, **112**, 219-235.
14. E. Guglielminotti, *Langmuir,* 1990, **6**, 1455-1460.
15. K. Pokrovski, K. T. Jung and A. T. Bell, *Langmuir*, 2001, **17**, 4297-4303.
16. S. Tada and S. Satokawa, *Catal. Commum.*, 2018, **113**, 41-45.
17. S. Tada, S. Kayamori, T. Honma, H. Kamei, A. Nariyuki, K. Kon, T. Toyao, K.-i. Shimizu and S. Satokawa, *ACS Catal.*, 2018, **8**, 7809-7819.
18. S. Tada, K. Fujiwara, T. Yamamura, M. Nishijima, S. Uchida and R. Kikuchi,

*Chem. Eng. J.*, 2020, **381**.

19. T. Liu, X. Hong and G. Liu, *ACS Catal.*, 2019, **10**, 93-102.
20. S. Tada, K. Larmier, R. Büchel and C. Copéret, *Catal. Sci. Tech.*, 2018, **8**, 2056-2060.
21. K. Samson, M. Śliwa, R. P. Socha, K. Góra-Marek, D. Mucha, D. Rutkowska-Zbik, J. F. Paul, M. R. Mikołajczyk, R. Grabowski and J. Słoczyński, *ACS Catal.*, 2014, **4**, 3730-3741.
22. C. Wu, L. Lin, J. Liu, J. Zhang, F. Zhang, T. Zhou, N. Rui, S. Yao, Y. Deng, F. Yang, W. Xu, J. Luo, Y. Zhao, B. Yan, X. D. Wen, J. A. Rodriguez and D. Ma, *Nat. Commun.*, 2020, **11**, 5767-5777.